RSC Advances

PAPER

View Article Online
View Journal | View Issue

Cite this: *RSC Adv.*, 2020, **10**, 2160

Characterization of biofuel production from hydrothermal treatment of hyperaccumulator waste (*Pteris vittata* L.) in sub- and supercritical water†

Jinbo Chen * and Songmao Li

In this study, hyperaccumulator waste, *i.e.*, *Pteris vittata* L. was converted into bio-oil, biogas and biochar *via* sub- and supercritical hydrothermal liquefaction processes. These products were characterized in terms of EI/MS, FTIR, TGA and GC to understand their chemical composition, thermal decomposition, structural properties and high biofuel reactivity. Characterization results revealed that the dominant chemical components in the heavy bio-oil were esters (40.22%), phenols (20.02%), alcohols (10.16%), organic acids (9.07%), nitrogenous compounds (8.83%) and ketones/aldehydes (6.42%), while the light oil was rich with a higher fraction of phenols (54.13%) and nitrogenous compounds (27.04%). Particularly, bio-oils obtained from supercritical conditions contained increased phenolic compounds and reduced oxygenated chemicals such as alcohols, aliphatic acid, ketones and aldehydes, suggesting the improved quality of bio-oil due to the reduction in oxygen contents. Meanwhile, H_2-rich syngas production with the H_2 yield of 38.87% was obtained at 535 °C for 20 min, and higher reaction temperature presented a positive influence on H_2 production during *Pteris vittata* L. liquefaction. Moreover, the remaining biochar product was analyzed to determine whether it could be used as a direct solid fuel or auxiliary fuel. This study provided full exploitation of this feedstock waste in energy and valuable chemical complexes.

Received 12th November 2019
Accepted 26th December 2019

DOI: 10.1039/c9ra09410e

rsc.li/rsc-advances

1. Introduction

Biobased feedstocks, including food crops, agricultural and forestry by-products, municipal wastes and algae biomass have been considered as some of the most potential energy sources to supplement conventional fossil fuel and valuable chemical feedstocks.[1–3] As a special type of lignocellulosic biomass with carbon-rich substances, hyperaccumulator biomass, which is used for the phytoremediation of heavy metal-contaminated soil, has attracted significant attention regarding its effective reutilization and reasonable disposal due to the large and annually increasing amount generated.[4,5] The efficient management and conversion of these hyperaccumulator wastes into series and high value of fuels and chemicals through appropriate process are urgently desiderate. Meanwhile, these huge quantities of hazardous biomass must be treated properly so that it does not cause any secondary contamination risk to the environment. Therefore, developing a reliable, effective and environment friendly technology to utilize these biomass wastes is important. Hydrothermal liquefaction (HTL) employing water or other solvent as working medium at mild reaction conditions has been demonstrated to be a promising thermochemical process to convert organic matters or wastes into valuable biofuels and chemicals with many advantages such as high energy efficiency, high product quality and mild reaction condition *etc.*[6–8] Through series of complex chemical reactions under sub- or supercritical conditions, the process converts diverse biomass feedstocks into four types of products, as shown in Scheme 1: energy-dense bio-crude oil with higher heating value (HHV) of up to 35–40 MJ kg^{-1};[9,10] biochar, which can be used as a solid fuel, adsorbent or catalysis support;[11,12] biogas (*e.g.*, combustible hydrogen and methane) and nutrient-rich aqueous products.[13] More importantly, during HTL process, particularly operating at pressures higher than 22.1 MPa and temperatures above 374 °C, the decomposition of organic substances in biomass could result in the release of heavy metals into the liquid phase and their subsequent translation into stable solid-phase fractions due to the changes in the water's physical properties (*i.e.*, its diffusivity, solubility, density and dielectric constant).[14,15] Thus, these advantages make HTL a suitable technique for treating hazardous biomass with particular value from an energy exploration and environmental protection standpoint. Research on HTL treatment of hyperaccumulator

Ningbo Institute of Materials Technology and Engineering, Chinese Academy of Sciences, Ningbo 315201, China. E-mail: jinbochen@nimte.ac.cn; Fax: +86-574-86685172; Tel: +86-574-86685172

† Electronic supplementary information (ESI) available. See DOI: 10.1039/c9ra09410e

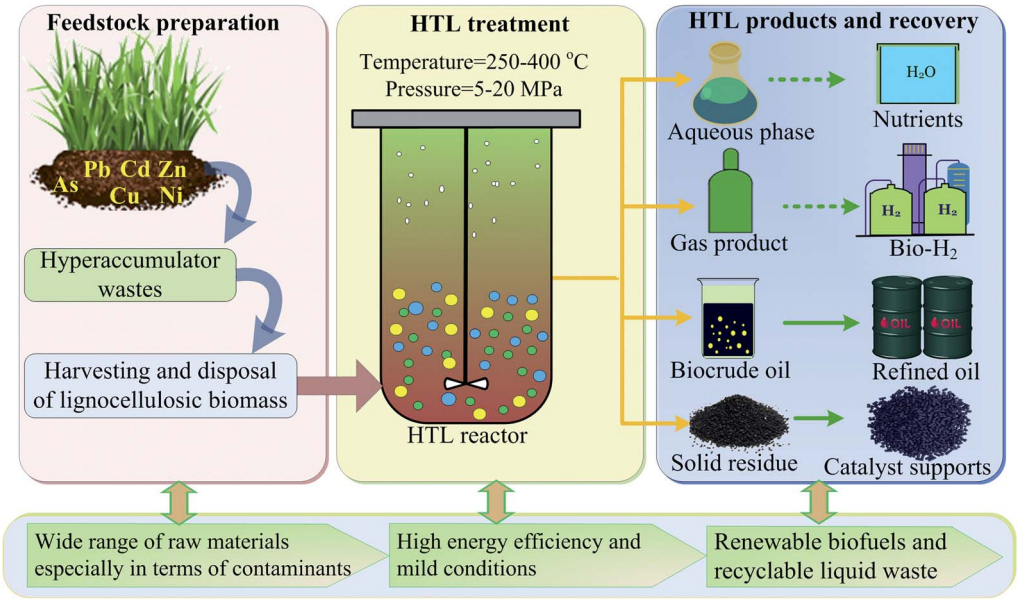

Scheme 1 Hydrothermal treatment of hyperaccumulator wastes with enriched heavy metals for the production of valuable biofuels and chemicals.

wastes have been carried out in recent years.[15–19] Clercq *et al.*[16] investigated the HTL process of *Pteris vittata* L. under sub- and supercritical conditions and demonstrated that the main products in the liquid phase were ketones and phenols. Yang *et al.*[17] employed hydrothermal process to obtain bio-oil and remove heavy metals from *Pteris vittata* L., and gained a bio-oil recovery efficiency of 83% with heavy metals removal efficiency of 99% under optimal condition. Recently, 21.5% yield of bio-oil with almost no heavy metals was obtained from hydrothermal conversion of *Sedum alfredii* Hance by Chen *et al.*[15] Investigation into the effect of inherent metals (such as lead, sodium and magnesium) on the chemical compositions in hydrothermal liquefaction of *Rhus chinensis* had also been carried out by Zhu *et al.*,[18] and it was found that these metals could improve the concentration of acetic and formic acids whereas decrease the content of levulinic acid. Besides, it was reported that during hydrothermal liquefaction of waste *Sedum plumbizincicola*, the released zinc ions could effectively promote the generation of acetic acid.[19]

Through these studies, it was found that hydrothermal liquefaction of hyperaccumulator wastes could result in a relatively high yield of bio-oil with higher calorific value. Meanwhile, the enriched heavy metals in the raw biomass could be converted to a stable state in the solid phase *via* HTL, which could be easily processed. More interestingly, it was found that metal ions such as lead, zinc and nickel might have synergistic catalytic effects in the production of bio-oil and the promotion of its quality. These results motivated us to explore the feasibility of converting *Pteris vittata* L. biomass to bio-oils with enhanced stability of enriched heavy metals *via* HTL process. However, most of the current researches about *Pteris vittata* L. wastes are concentrated in the recovery of heavy metals or the yield of bio-oils during subcritical HTL process, and little is known with regard to chemical transformation of bio-oils between sub- and supercritical conditions. Furthermore, a wide range of physicochemical properties such as chemical composition, thermal decomposition, structure property and elemental composition of bio-oils under both sub- and supercritical conditions is very important to identify its potential applications as fuels. Meanwhile, these properties can also provide important indications for both the optimization of reaction parameters and the improvement of purification methods for their further exploitation as an alternative fuel. To date, however, no such comprehensive characterizations on bio-oil as well as biochar and gaseous products produced from *Pteris vittata* L. liquefaction have been performed. In a previous work,[20] we conducted subcritical hydrothermal conversion of *Pteris vittata* L. into bio-oils with a maximum yield of 16.88% and energy recovery efficiency of 45.10%. Additionally, we demonstrated that bio-oils were composed of esters, phenols, alcohols, ketones and acids based on GC-MS analysis. However, chemical characterization of bio-oils produced under supercritical conditions was not presented and needed further investigation. Besides, there was no more comprehensive work concerning the properties (such as thermal decomposition, structure property and energy density) of these bio-oils, biochar and gaseous products derived from *Pteris vittata* L. liquefaction under both sub- and supercritical conditions. In the current study, hyperaccumulator waste, *i.e.*, *Pteris vittata* L. was converted to bio-oil, biogas and biochar by hydrothermal liquefaction process in both sub- and supercritical water. These products were further characterized in terms of gas chromatography-mass spectrometry (GC-MS), Fourier transform infrared spectroscopy (FTIR), thermogravimetric measurements (TGA) and gas chromatography (GC) to understand their various chemical, physical properties, thermal

decomposition and their high biofuel reactivity. Moreover, the energy density of bio-oils and bio-chars was represented using a Van Krevelen diagram in terms of their H/C and O/C ratios. This study may provide a novel contribution to the complete understanding of the physicochemical properties of biofuel products from hydrothermal treatment of *Pteris vittata* L. and a full exploitation of this feedstock waste in energy and valuable chemical complexes.

2. Materials and methods

2.1 Biomass feedstock

P. vittata L. feedstock were dried in drier at 105 °C overnight and then grounded into uniform particle size of less than 100 mesh. The contents of carbon, moisture, ash and volatilization were 6.35, 60.69, 20.58 and 18.73 wt%, respectively.[20] In addition, the contents of carbon, hydrogen, oxygen and nitrogen were 51.49, 6.50, 38.06 and 3.54 wt%, respectively.[20] Notably, these samples had high concentrations of heavy metals, such as arsenic, copper, lead, nickel, cadmium and chromium, while arsenic, zinc and nickel were the main components with concentrations of 8547 mg kg^{-1}, 225 mg kg^{-1} and 176 mg kg^{-1}, respectively. It has recently been reported that released metal ions such as nickel, zinc, copper and lead presented remarkable impact on the HTL reactions and could improve the bio-oil yield and promote product quality.[19,21,22]

2.2 HTL procedure and analysis methods

A schematic diagram of the experimental setup and procedure for the separation of the HTL products was shown in Fig. 1. HTL runs were conducted in a 500 mL double-walled batch reactor made of hastelloy. The reaction temperature inside the reactor was maintained by a power supplier with a 2.0 kW capacity at an average heating rate of 5 °C per minute. 10 g of raw biomass was mixed completely with 100 mL of deionized water, resulting in a concentration of 9.1 wt%. Then, the whole system was purged with nitrogen gas for air replacement and maintained at an initial pressure of 2.0 bar. After a 15 min residence time, the reactor was rapidly quenched to normal temperature by both an internal cooling coil and an external electronic fan at a cooling rate of 9 °C per min. The operating temperatures employed in this study included both subcritical conditions (250–350 °C) and supercritical conditions (390–535 °C). After hydrothermal treatment, the gaseous products were vented and collected in gas sampling bags for further gas composition tests. The liquid–solid mixture was separated with vacuum distillation and the solid phase was then extracted with acetone for the separation of acetone-soluble and acetone-insoluble compounds. Solid residues were obtained by drying the acetone-insoluble fraction in drier at 105 °C for 12 hours. The heavy oil was obtained by removing the acetone from the acetone-soluble fraction in a rotating evaporator at 35 °C and 2 mbar. Dichloromethane (DCM) was finally added to the liquid filtrate for the separation of the DCM-soluble (*i.e.* the light oil) and DCM-insoluble phases (*i.e.* the aqueous product).

The oil products from liquefaction process were subject to GC-MS system (Shimadzu QP2010, Japan) using an electron impact (EI) ionization equipped with an HP-5MS column. Functional group information was derived from FT-IR spectrometer (Thermo Nicolet Nexus 410, USA) within a spectral range of 400–4000 cm^{-1} at a resolution of 2.0 cm^{-1}. The gas compositions were analyzed by GC (Agilent-490, USA) with an MS-5A packed column for H_2, CH_4 and CO and a PPU capillary column for CO_2. The thermal decomposition behavior was examined by a TGA analyzer (Mettler-Toledo TGA/DSC3, Switzerland) with a heating rate of 10 °C per minute from 40–700 °C.

3. Results and discussion

3.1 Chemical properties of the bio-oil

3.1.1 Chemical compositions of the bio-oil. It has been demonstrated that the main chemical compositions in bio-oils generated from the hydrothermal treatment of *P. vittata* L. under subcritical conditions are esters and alcohols (making up approximately 50% of the total area), followed by ketones, acids, phenols, hydrocarbons and amides in varying contents depending on the operating temperature.[20] To further identify these products under supercritical conditions, an extensive study was performed in which the chemical compositions of both the heavy and light oils (Table 1 below) derived from *P. vittata* L. liquefaction at 390 °C were presented based on the GC-MS analysis and presented in Table 1. Four types of major components in the heavy bio-oil according to their functional groups could be classified as follows:[23,24] polyphenols (phenols and their derivatives), oxygenates (esters, alcohols, ketones, aldehydes and aliphatic acids), nitrogenous compounds (nitriles and amines) and hydrocarbons. In the heavy oils, seven phenolic compounds were consecutive identified as 4-ethylphenol (5.24%), *m*-cresol (4.53%), *o*-xylene-3,6-diol (2.64%), phenol (2.51%), 3-ethyl-5-methylphenol (2.10%), 2-ethylphenol (1.59%) and 2-ethyl-4-methylphenol (1.41%). These components accounted for about 20.02% of the total area. In the oxygenated compounds, the esters were the most abundant with 40.22% of the total chromatographic area, including L-ascorbyl dipalmitate (26.22%), 3,7,11,15-tetramethyl-hexadecyl ester (7.52%), heptadecyl octanoate (4.49%) and 14-tricosen-1-yl formate (4.49%). Furthermore, the heavy bio-oil exhibited a large presence of substituted alcohols such as 2-methyl-2-hexanol (5.07%) and γ-sitosterol (3.05%), aliphatic acids such as palmitoleic acid (6.20%) and stearic acid (2.87%), and ketones or aldehydes (6.42%) such as sitostenone. Little amounts of nitrogenous compounds (8.83%) and hydrocarbons (5.29%) were also detected in the heavy oil. Compared with characterization results obtained under subcritical hydrothermal conditions,[20,25,26] one of the most distinct properties of bio-oil derived from supercritical condition was a significant reduction of selected ketones, aldehydes, alcohols and aliphatic acids with an increased content of certain phenols and esters. It was reported that polyphenols presenting in bio-oil were mainly produced from the degradation of lignin through cleavage reactions or cracking of ether-bonds in the raw feedstock.[27,28] However, lignin compound was difficult to degrade even at

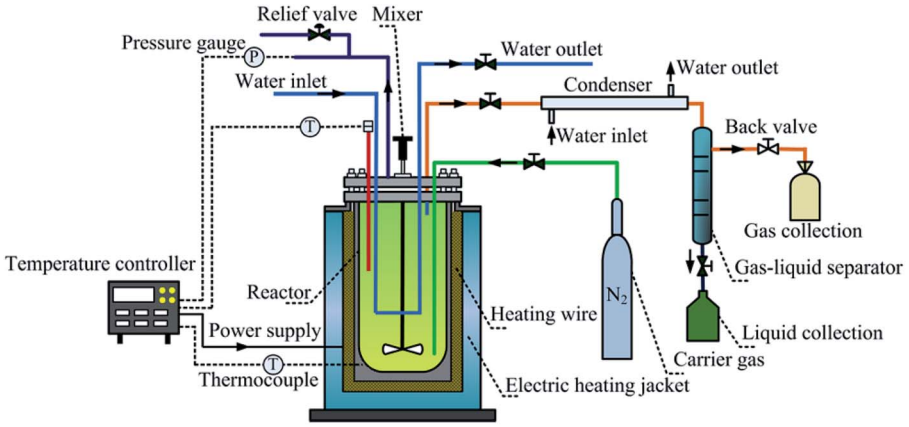

(a) Schematic illustration of HTL setup.

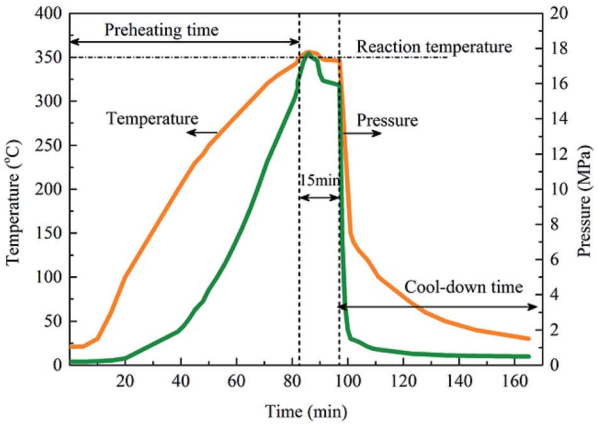

(b) Typical temperature and pressure profile at 350 °C with a 15min retention time.

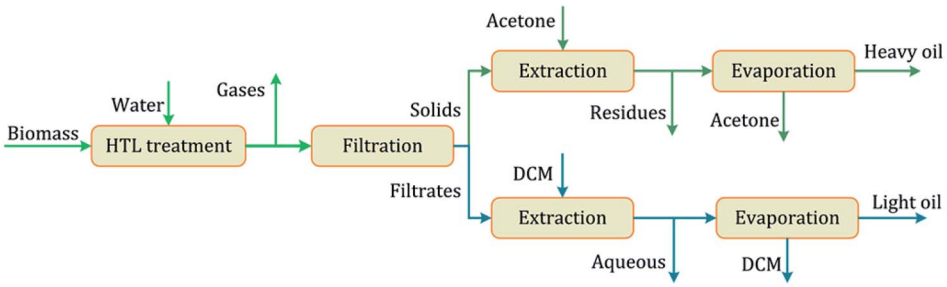

(c) Simplified separation process of the HTL products.

Fig. 1 Experimental setup and separation procedure for the HTL runs.

relative high temperature (250–350 °C) due to its high degree of polymerization and complex branching.[29,30] Clearly, supercritical temperature of 390 °C employed in this study effectively improved lignin degradation and produced more phenolics compounds, thus realizing high conversion efficiency and selectivity of lignin to polyphenols. The results demonstrated the suitability of bio-oils *via* hydrothermal liquefaction of *P. vittata* L. biomass for conversion into renewable fuels and chemical feedstocks. For example, phenolic compounds could be employed for producing aromatic chemicals or transportation fuels after further upgrading through hydrotreating.[24] Besides, results from Table 1 illustrated that the amount of ketones, aldehydes, alcohols and aliphatic acids decreased to 25.65% of total compounds after supercritical hydrothermal treatment,[20] compared with 41.18–60.24% for those products derived from subcritical conditions. This result suggested that these oxygenated compounds could be broken down into gaseous products in the form of carbon monoxide and carbon

Table 1 Major compounds identified by GC-MS in heavy and light oils produced from HTL of *P. vittata* L. at 390 °C

	Chemical compounds				Relative abundance[a] (area, %)	
No.	RT[b] (min)	Type	Formula	MW[c]	HO[d]	LO[e]
Ketones/aldehydes					**6.42**	**7.21**
1	6.730	2,3-Dimethyl-2-cyclopenten-1-one	$C_7H_{10}O$	110	1.85	—[f]
2	8.250	1-Acetyl-1-cyclohexene	$C_8H_{12}O$	124	1.47	—
3	14.010	β-Cyclocitral	$C_{10}H_{16}O$	152	—	1.14
4	14.525	4-(1,3,3-Trimethyl-bicyclo[4.1.0]hept-2-yl)-but-3-en-2-one	$C_{14}H_{22}O$	206	—	2.67
5	15.125	(3*E*)-4-(2,6,6-Trimethyl-1-cyclohexen-1-yl)-3-penten-2-one	$C_{14}H_{22}O$	206	—	2.40
6	25.555	Cyclopentadecanone, 2-hydroxy	$C_{15}H_{28}O_2$	240	1.32	—
7	37.000	Sitostenone	$C_{29}H_{48}O$	412	1.78	—
8	37.050	β-Sitostenone	$C_{29}H_{48}O$	412	—	1.00
Phenols					**20.02**	**54.13**
9	6.525	Phenol	C_6H_6O	94	2.51	—[g]
10	8.030	*m*-Cresol	C_7H_8O	108	4.53	—
11	9.160	2-Ethylphenol	$C_8H_{10}O$	122	1.59	—
12	9.760	4-Ethylphenol	$C_8H_{10}O$	122	5.24	1.13
13	10.310	Catechol	$C_6H_6O_2$	110	—	16.88
14	10.780	3-Ethyl-5-methylphenol	$C_9H_{12}O$	136	2.10	—
15	10.970	2-Ethyl-4-methylphenol	$C_9H_{12}O$	136	1.41	—
16	11.890	4-Methylcatechol	$C_7H_8O_2$	124	—	12.74
17	12.690	4-Ethylresorcinol	$C_8H_{10}O_2$	138	—	3.89
18	13.335	*o*-Xylene-3,6-diol	$C_8H_{10}O_2$	138	2.64	3.22
19	13.340	4-Ethylbenzene-1,2-diol	$C_8H_{10}O_2$	138	—	13.86
20	14.695	4-Propylresorcinol	$C_9H_{12}O_2$	152	—	2.41
Alcohols					**10.16**	**7.83**
21	4.580	2-Methyl-2-hexanol	$C_7H_{16}O$	116	5.07	7.83
22	18.035	3,7,11-Trimethyldodecan-1-ol	$C_{15}H_{32}O$	228	2.04	—
23	41.135	γ-Sitosterol	$C_{29}H_{50}O$	414	3.05	—
Esters					**40.22**	**1.40**
24	14.935	Heptadecyl octanoate	$C_{25}H_{50}O_2$	382	4.49	—
25	16.145	Ethyl-7-oxo-1,3,4,5,6,7-hexahydro-4*a*(2*H*)-naphthalenecarboxylate	$C_{13}H_{18}O_3$	222	—	1.40
26	17.910	3,7,11,15-Tetramethyl-hexadecyl ester	$C_{22}H_{44}O_2$	340	7.52	—
27	21.445	L-Ascorbyl dipalmitate	$C_{38}H_{68}O_8$	652	26.22	—
28	30.630	14-Tricosen-1-yl formate	$C_{24}H_{46}O_2$	366	1.99	—
Hydrocarbons					**5.29**	—
29	19.225	3,7,11,15-Tetramethyl-2-hexadecene	$C_{20}H_{40}$	280	3.72	—
30	29.045	9-Hexacosene	$C_{26}H_{52}$	364	1.57	—
31	39.765	Pentatriacont-17-ene	$C_{35}H_{70}$	490	1.40	—
Organic acids					**9.07**	**2.38**
32	14.240	(4-Glycoloylphenoxy)acetic acid	$C_{10}H_{10}O_5$	210	—	2.38
33	25.560	Palmitoleic acid	$C_{16}H_{30}O_2$	254	6.20	—
34	26.095	Stearic acid	$C_{18}H_{36}O_2$	284	2.87	—
N-containing compounds					**8.83**	**27.04**
35	8.895	3-Hydroxy-2-methylpyridine	C_6H_7NO	109	—	2.91
36	9.575	3-Hydroxy-6-methylpyridine	C_6H_7NO	109	—	3.30
37	9.825	2,6-Dimethyl-3-hydroxypyridine	C_7H_9NO	123	—	5.22
38	10.220	2-(3-Furyl)-4-methyl-5-phenyl-1,3-oxazolidine	$C_{14}H_{15}NO_2$	229	—	4.15
39	13.440	2,3-Dimethyl-2,3-diphenylbutanedinitrile	$C_{18}H_{16}N_2$	260	4.52	—
40	18.170	(1*E*)-2-Methyl-*N*-(2-phenylethyl)-1-butanimine	$C_{13}H_{19}N$	189	—	1.19
41	21.065	5,10-Diethoxy-2,3,7,8-tetrahydro-1*H*,6*H*-dipyrrolo[1,2-*a*:1′,2′-*d*]pyrazine	$C_{14}H_{22}N_2O_2$	250	—	2.51
42	30.230	Oleamide	$C_{18}H_{35}NO$	281	4.31	—
43	30.235	*cis*-13-Docosenoamide	$C_{22}H_{43}NO$	337	—	3.29

[a] Obtained by the peak area normalization method. [b] RT: retention time. [c] MW: molar weight. [d] HO: heavy oil. [e] LO: light oil. [f] No detection. [g] Components with peak area values less than 1.0%.

dioxide, which were preferred products under supercritical conditions. More importantly, the reduction in contents of oxygenated compounds improved the bio-oil quality with low nitrogen and oxygen contents.[24]

The major compounds existing in the light bio-oil were quite similar with those in the heavy oil, however, obvious differences could be observed in terms of their contents. The light oil consisted of lower carbon compounds (C_4–C_{14}) with higher fraction of phenols (54.13%), whereas the ester content was greatly decreased to 1.40% in comparison to 40.22% in the heavy oil. Similar results were reported in many previous studies on bio-oil production during HTL treatment of lignocellulosic biomass.[23,31–33] In addition, a higher content of nitrogenous compounds (27.04%) was detected in the light oil, indicating that more nitrogen element in the raw biomass was migrated into the light bio-oil during supercritical HTL process.

3.1.2 Structure properties of bio-oil determined using FTIR spectroscopy. The structural properties related with functional groups of the heavy oils derived from FT-IR analysis and spectral band assignments (cyan bars) was compared in Fig. 2. Significant absorbance peaks corresponding to C–H_n stretching vibrations (3000–2800 cm^{-1}) and C–H bending vibrations (1457 cm^{-1} and 1383 cm^{-1}) were observed for all samples, consistent with the alkanes and aromatic compounds identified by GC-MS analysis, illustrating high amounts of carbon and hydrogen in heavy oils.[26,34] The C=C stretching vibration peak at 1615 cm^{-1} also suggested the presence of aromatic alkanes in the heavy oils.[35] The broad O–H stretching vibrations at 3407 cm^{-1} corresponded to hydroxyl functional groups in phenols, alcohols and acid compounds.[36,37] The FT-IR absorptions between 1300 cm^{-1} and 950 cm^{-1} could be caused by C–O stretching vibrations and O–H bending vibrations, respectively, suggesting the presence of esters, acids, phenols and alcohols.[38,39] Moreover, the N–H bending vibration peak at 1514 cm^{-1} corresponded to nitrogenous compounds, while the absorbance peak at 808 cm^{-1} indicated the possible presence of aromatic compounds.[39] These results demonstrated the presence of various components identified by GC-MS in the heavy oils, such as phenols, hydrocarbons, alcohols, acids and nitrogenous compounds. Notably, the vibration intensity of C–H group decreased with the increase of reaction temperature from 300 °C to 350 °C, suggesting the further decomposition of alkanes and aromatic compounds with elevated temperature. In addition, the peak intensity of C–O vibrations was significantly decreased and almost disappeared at 350 °C, indicating that some main components, such as esters, were hydrolyzed completely at 350 °C.

3.1.3 Thermal decomposition behaviors of bio-oil determined using TGA analysis. The results from TG/DTG analysis were helpful in demonstrating thermal decomposition behaviors of bio-oil during the HTL process. As presented in Fig. 3, heating the heavy oils to 700 °C in nitrogen atmosphere resulted in a total weight loss of approximately 70–88% under all conditions. The weight loss of the heavy oils before 150 °C was less than 7% for all samples, which was due to the volatilization of light components in the heavy oils. Then, the major weight loss (65–87%) occurred in the temperature range from 150 to 475 °C, representing the decomposition and volatilization of

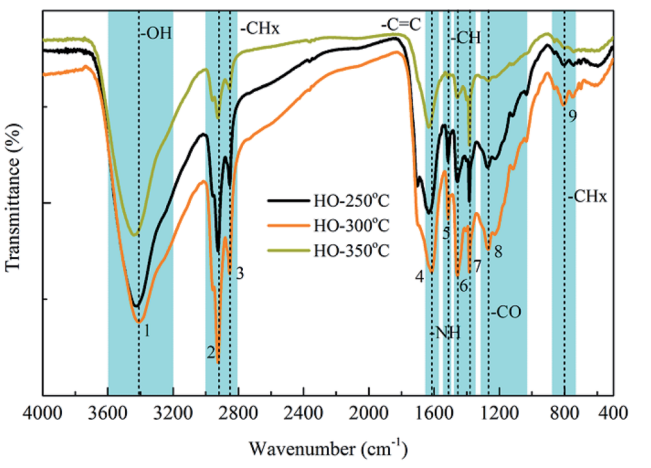

Fig. 2 FTIR spectra of heavy oils produced at various reaction temperatures. (1) 3407 cm^{-1}; (2) 2925 cm^{-1}; (3) 2853 cm^{-1}; (4) 1615 cm^{-1}; (5) 1514 cm^{-1}; (6) 1457 cm^{-1}; (7) 1383 cm^{-1}; (8) 1268 cm^{-1}; (9) 808 cm^{-1}.

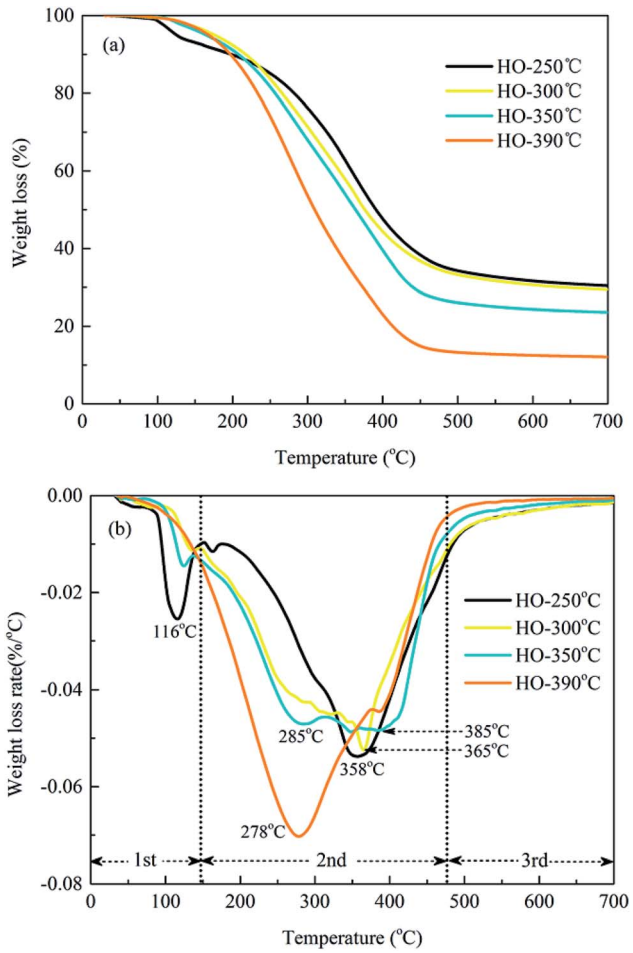

Fig. 3 TG-DTG curves of heavy oils produced at different HTL temperatures. (a) TG curves; (b) DTG curves.

diesel and similar lubricating oil fractions for ships or engines.[40,41] Moreover, the operating temperature had great effect on the thermal decomposition properties of the heavy oils. The maximum weight loss increased from 70% to 88% as the HTL temperature increased from 250 °C to 390 °C, implying that higher temperature favored the production of lighter biodegradable matter. This would favor for further upgrading or refining to commercial fuels and chemicals with reduced heating demands. Moreover, the heavy oils obtained at lower HTL temperatures (250 °C and 300 °C) had maximum weight loss rates at approximately 358 °C and 365 °C, respectively, while the heavy oil obtained at higher HTL temperature (350 °C) showed obvious two weight loss peaks at 285 °C and 385 °C, indicating the volatilization of both lighter and heavier components, respectively, during the HTL process. These results were in agreement with test results obtained in the previous discussion,[20] which revealed that at higher HTL temperatures (>350 °C), the bio-oils underwent secondary degradation and repolymerization reactions to form smaller and larger molecular components, respectively. Furthermore, it was interesting to note that the bio-oil obtained at 390 °C presented a lower weight loss peak at approximately 278 °C with a greater weight loss rate of 0.07% with each degree. The specific thermal decomposition behavior of heavy oils produced from supercritical conditions above 375 °C was closely related to the unique ability and properties of supercritical water, such as high thermal conductivity, low dielectric constant and weak viscosity, which would enhance the chemical conversion of biomass to small liquid and gaseous components with high efficiency.[30,42]

3.2 Characteristics of HTL biochars

3.2.1 Structure properties of biochar determined using FTIR spectroscopy. The FTIR spectra of the raw biomass and solid residues produced at different operating temperatures were shown in Fig. 4. There was an obvious decrease in the intensity of the absorbance peaks due to O–H (3440 cm^{-1}) and C–H (3000–2800 cm^{-1}) vibrations with increasing operating temperatures compared to those of the raw biomass, indicating the loss of hydroxyl, carboxyl and methylene groups in the raw biomass after the HTL process. These results were consistent with the previous results of hydrothermal treatment of barley straw biomass within range of 280–400 °C.[24] The reduction of these peaks was possibly caused by the occurrence of dehydration or decarboxylation reaction of the main polymers in the raw biomass, in accordance with the decrease in the fixed carbon and hydrogen contents in the solid residues with elevated temperature. In contrast, the absorbance peak located at 1384 cm^{-1}, which was tentatively assigned to C–H bending vibrations, became more significant with increasing temperatures, partially indicating that alkane structures were possibly formed during the HTL process. Moreover, the intensity of the absorbance peak at 1062 cm^{-1}, related to C–O bending vibrations, significantly decreased after the HTL process as the operating temperature increased, resulting in fewer oxygen-containing groups than in the raw biomass. It was interesting to note that all solid residues after the HTL process had no absorbance peak at 1243 cm^{-1} due to C–O stretching vibrations, suggesting the absence of acids, alcohols or ester groups in the solid residues.

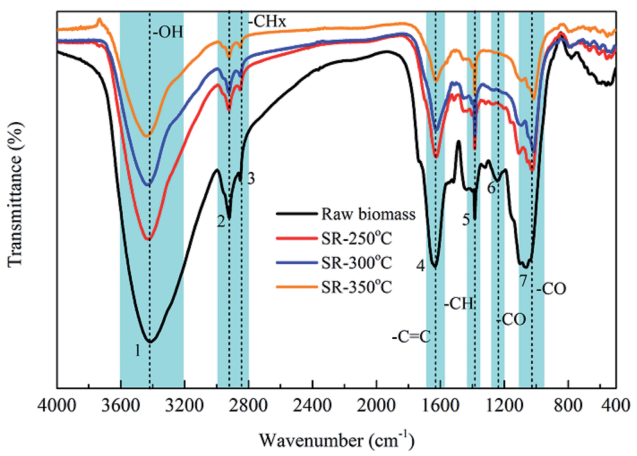

Fig. 4 FTIR spectra of raw biomass and biochars produced from at various HTL temperatures. (1) 3440 cm^{-1}; (2) 2923 cm^{-1}; (3) 2852 cm^{-1}; (4) 1626 cm^{-1}; (5) 1384 cm^{-1}; (6) 1243 cm^{-1}; (7) 1062 cm^{-1}.

3.2.2 Thermal decomposition behaviors of biochar using TGA analysis. The thermal decomposition properties of the raw biomass and solid residues obtained from TG/DTG analysis at different HTL temperatures were presented in Fig. 5. The whole decomposition process could be characterized by three typical weight loss stages, *i.e.*, dehydration, devolatilization and residue decomposition based on the rate of weight loss.[43] The raw biomass remained relatively stable without thermal degradation up to 170 °C, which was attributed to the loss of free water from the raw materials (approx. 7%). Then, the weight loss (approx. 60%) was happened mainly in the second stage (180–414 °C) with a maximum degradation peak at 311 °C, where higher temperature caused the significant volatilization or decomposition of hemicellulose, cellulose and some lignin.[44] Finally, a slight weight loss of 38% of the final residue was observed when the temperature exceeded 560 °C, corresponding to the slow decomposition of remaining lignin and macromolecular components from the previous stage. Comparatively speaking, the thermal degradation behavior of the biochars was apparently different from those of the raw biomass. The TG/DTG curves presented almost no weight loss in the first stage due to the drying of the solid residues after HTL treatment. In the second stage, the main devolatilization occurred within the temperature range of 320–530 °C and the weight loss decreased from 36% to 16% with elevated HTL temperature, suggesting that most of the biodegradable components in the raw biomass were decomposed and transformed into bio-oil or gaseous products after the HTL process, while the rest consisted of fixed carbon and ash. Moreover, the DTG curves presented increased volatilization peaks from 429 °C to 449 °C with HTL treatment temperature ranging from 250 °C to 390 °C, indicating stronger degradation ability of hemicelluloses, cellulose and even some lignin with elevated temperature in the HTL process. Therefore,

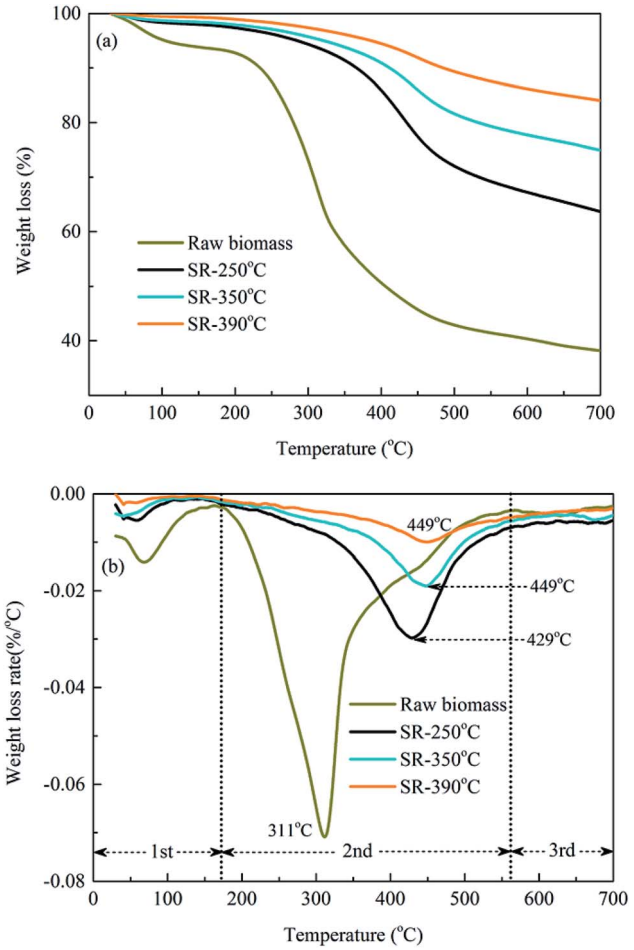

Fig. 5 TG and DTG curves of the original biomass and solid residues obtained at 250 °C, 350 °C and 390 °C. (a) TG curves; (b) DTG curves.

the HTL biochars exhibited strong thermal stability at high decomposition temperatures in comparison to that of the raw biomass, which could help decrease the leaching of organic pollutants and improve the immobility of the enriched heavy metals.[45]

3.3 Components of gaseous products determined using GC analysis

Based on the unique ability and properties of supercritical water, the production of hydrogen from biomass *via* the HTL process, *i.e.*, hydrothermal gasification is a currently popular area of research and represents a potential renewable biogas resource for the future.[46] To reveal the influence of operating temperatures on the hydrothermal conversion of *Pteris vittata* L. into gaseous production, the gas yields and compositions produced from *Pteris vittata* L. liquefaction were studied under supercritical conditions within a wide temperature range of 380–535 °C with a fixed operating pressure (23 MPa), residence time of 20 min and solid-to-liquid ratio of 1 : 40. As presented in Fig. 6, at the outlet of the hydrothermal process, a gaseous mixture mainly consisting of H_2, CH_4, CO, CO_2 and small amounts of C_2H_4 and C_2H_6 was detected. Furthermore, higher reaction temperature had a positive influence on higher H_2 production during HTL process. With increasing operating temperature from 380 °C to 535 °C, the yield of the H_2 fraction significantly increased from 6.45% to 38.87%, while the CO_2 yield dropped drastically from 86.06% to 34.69%, especially beyond 495 °C. The predominant effect of reaction temperatures on H_2 production during hydrothermal process was also reported in literatures.[47] The yield of the CH_4 fraction increased with elevated temperature, except that a drop of 22.41% occurred at 535 °C. Moreover, the yield of the CO fraction increased from 2.47% to 4.27% with temperature increasing from 380 °C to 430 °C and then decreased gradually to 1.83% with further elevated temperature of 535 °C. In addition, only a small amount of C_2H_6 (0.78–3.20%) and C_2H_4 (0.25–0.47%) were obtained during HTL process and the contents of these compounds presented a similar tendency with increasing temperature to that of CO. In the present study, the yields of H_2 and CO_2 presented a monotonic variation tendency with increasing temperatures. Similar results were obtained in a low temperature range of 300–445 °C.[20] However, the CO and CH_4 yields showed opposite behaviors at higher temperatures (above 535 °C in this study) than that at low temperatures. These results was caused by the significant decrease in the dielectric constant of water at supercritical temperature.[48] Importantly, the final gaseous yields were also believed to be the result of a series of complex and competing chemical reactions closely related to the operating temperatures.[49] The reforming reaction was an endothermic reaction, which would be enhanced at elevated temperatures, resulting in a drastic increase in H_2 and CO yields.[50] Moreover, the methanation reaction and water–gas reaction were promoted with increasing temperatures, resulting in the conversion of CO to CH_4, CO_2 and H_2. The decreased yield of CO above 430 °C was due to the consumption of CO in the water–gas shift reaction. Furthermore, it should be noted that the varying gaseous yields with temperature indicated that competitive reaction pathways dominated at different temperature ranges.

3.4 Investigation into the reaction pathway of HTL

To better examine the variation in the atomic compositions and related reaction pathways during the HTL treatment of *P.*

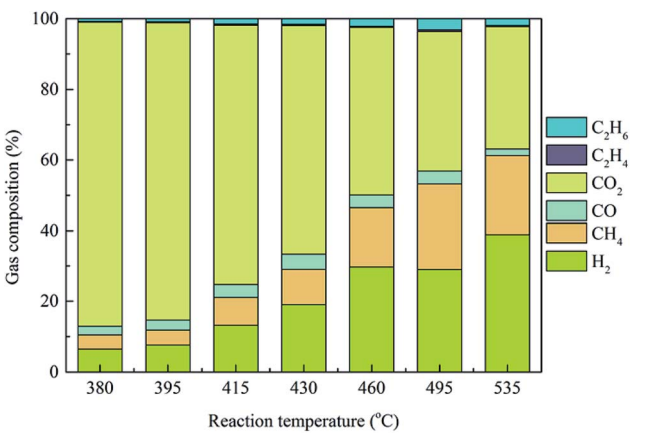

Fig. 6 Gas yields and compositions under various operating temperatures during HTL process.

vittata L., the bio-oils and biochars obtained at various HTL temperatures were classified in terms of their H/C and O/C ratios in a Van Krevelen diagram, as illustrated in Fig. 7. The H/C and O/C ratios for petroleum, biodiesel, lignite, bituminous and anthracitic coals were illustrated for comparison. The H/C and O/C ratios of the raw material were also reported as a control. The high temperatures employed in this work were beneficial for the improvement of the bio-oil quality but not advantageous for the solid residues. In contrast to the raw biomass, the corresponding H/C and O/C ratios (H/C, 1.26–1.46; O/C, 0.16–0.28) of the bio-oils were located in the region adjacent to petroleum or biodiesel fuels (H/C, 1.45–1.93), indicating the potential applications of these bio-oils as substitute fuels after further upgradation because of its higher energy density. Then, both the H/C and O/C ratios substantially decreased from 1.51 to 1.26, and 0.55 to 0.24, respectively when the operating temperature was increased from 250 °C to 300 °C, strictly following the dehydration and decarboxylation line. These results illustrated that dehydration and decarboxylation reactions in the bio-oils might be enhanced in this temperature range. Moreover, the observed CO_2 and CO contents in the gaseous products indirectly proved the existence of decarboxylation and dehydration reactions during the HTL process. As the reaction temperature rised from 300 °C to 390 °C, the O/C ratio continuously decreased from 0.24 to 0.16, whereas the H/C ratio started to increase from 1.26 to 1.46. This finding implied that oxygen was substantially removed from solid residues during HTL process with elevated temperature, while hydrogen was initially removed from the biomass at temperatures below 300 °C and then hydrogenating reaction occurred at higher temperatures. As the operating temperature rised from 250 °C to 390 °C, the H/C ratio in the biochar decreased from 1.15 to 0.84 and the O/C ratio increased slightly from 0.95 to 1.07, suggesting that demethanation was a dominant pathway for biochar formation during HTL. Moreover, a slight deviation from the demethanation line was presented in the SR-300 °C sample and a decreased O/C ratio with constant H/C ratio was observed, suggesting that dehydration reaction might be involved at higher temperatures. These results were consistent with the FTIR analysis of the raw biomass and solid residues presented in Section 3.1.1 that O–H and C–H vibrations in the biomass decreased with elevated temperature due to the occurrence of dehydration and demethanation reactions. In addition, it was noteworthy that the O/C ratios of the biochars (0.93–1.07), even those obtained at the relatively low temperature of 250 °C, were significantly higher than that of the lignite coal (H/C, 1.2; O/C, 0.3) used in the present study, which would cause the elemental composition of the biochars to deviate far from that of lignite coal.

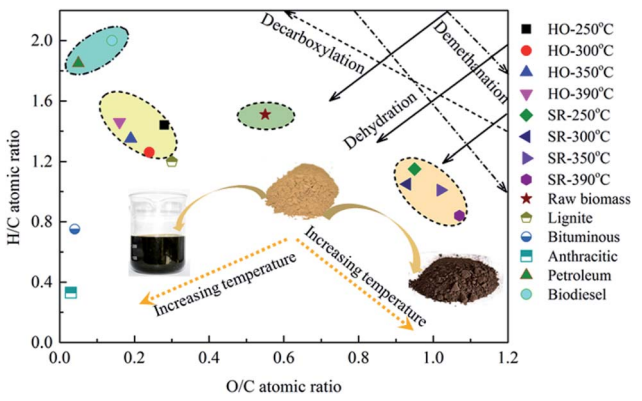

Fig. 7 Van Krevelen diagram for *Pteris vittata* L. and HTL products obtained from different temperatures in comparison with other types of fuels (lignite, bituminous, anthracitic coals, petroleum and biodiesel oils). The lines represent dehydration, decarboxylation and demethanation pathways.

4. Conclusions

In this study, hyperaccumulator waste, *i.e.*, *Pteris vittata* L. was converted to bio-oil, biogas and biochar *via* hydrothermal treatment under both sub- and supercritical conditions. Characterization results showed that the major chemical components of bio-oil were C_6–C_{28} organic compounds including esters, phenols, alcohols, fatty acids, ketones and aldehydes which are also components of crude oil, indicating that the bio-oils can be utilized as alternatives to fossil fuels or valuable chemicals with great potential. The ratios of H/C and O/C (1.26–1.46 and 0.16–0.28) were within the biodiesel range (H/C, 1.45–1.93), which also demonstrated its potential as a potential source for energy because of its higher energy density. More importantly, the reduction of contents in oxygenated chemicals resulted in an improved quality of bio-oil due to the reduction in oxygen contents. Another important achievement in this study was that within the range of operating parameters, H_2-rich syngas production with the H_2 yield of 38.87% was obtained at 535 °C for 20 min. This research indicated the effective utilization of HTL to handle *Pteris vittata* L. waste for the production of high value gaseous fuel and also demonstrated the positive effect of higher reaction temperature on the higher H_2 production. For the remaining biochar product, it had higher O/C values (0.93–1.07) comparable to lignite (O/C, 0.3) at all reaction temperatures, suggesting that the produced biochars were not appropriate for direct combustion or as solid biofuels. However, it was gratifying to find that the thermal stability of these solid products was obviously enhanced after HTL treatment, which could help decrease the leaching capacity of organic pollutants and promote stabilization of the enriched heavy metals.

Conflicts of interest

The authors declare no competing financial interest.

Acknowledgements

The authors would like to acknowledge the financial support from the Natural Science Foundation of Zhejiang Province, China (No. LY18E060001) and the experimental support from NIT. The authors are also grateful to Ms Yingying Han in NIMTE for help on analysis of the products.

References

1 M. Parsa, H. Jalilzadeh, M. Pazoki, R. Ghasemzadeh and M. Abduli, *Bioresour. Technol.*, 2018, **250**, 26–34.
2 S. C. Yim, A. T. Quitain, S. Yusup, M. Sasaki, Y. Uemura and T. Kida, *J. Supercrit. Fluids*, 2017, **120**, 384–394.
3 A. Aierzhati, M. J. Stablein, N. E. Wu, C.-T. Kuo, B. Si, X. Kang and Y. Zhang, *Bioresour. Technol.*, 2019, **284**, 139–147.
4 D.-X. Zhong, Z.-P. Zhong, L.-H. Wu, H. Xue, Z.-W. Song and Y.-M. Luo, *Fuel Process. Technol.*, 2015, **131**, 125–132.
5 K. Krzciuk and A. Gałuszka, *Crit. Rev. Biotechnol.*, 2015, **35**, 522–532.
6 J. Arun, P. Varshini, P. K. Prithvinath, V. Priyadarshini and K. P. Gopinath, *Bioresour. Technol.*, 2018, **261**, 182–187.
7 Z. Zhu, L. Rosendahl, S. S. Toor and G. Chen, *Sci. Total Environ.*, 2018, **630**, 560–569.
8 K. R. Arturi, S. Kucheryavskiy and E. G. Søgaard, *Fuel Process. Technol.*, 2016, **150**, 94–103.
9 K. Kapusta, *Waste Manag.*, 2018, **78**, 183–190.
10 N. Shamsul, S. K. Kamarudin and N. A. Rahman, *Renewable Sustainable Energy Rev.*, 2017, **80**, 538–549.
11 A. Saba, P. Saha and M. T. Reza, *Fuel Process. Technol.*, 2017, **167**, 711–720.
12 S. F. Hashmi, H. Meriö-Talvio, K. J. Hakonen, K. Ruuttunen and H. Sixta, *Fuel Process. Technol.*, 2017, **168**, 74–83.
13 T. Muppaneni, H. K. Reddy, T. Selvaratnam, K. P. R. Dandamudi, B. Dungan, N. Nirmalakhandan, T. Schaub, F. O. Holguin, W. Voorhies and P. Lammers, *Bioresour. Technol.*, 2017, **223**, 91–97.
14 M. N. Islam and J.-H. Park, *J. Environ. Manage.*, 2017, **191**, 172–178.
15 H. Chen, X. Wang, X. Lyu, L. Xu, J. Wang and X. Lu, *J. Environ. Chem. Eng.*, 2019, **7**, 103321.
16 M. Carrier, A. Loppinet-Serani, C. Absalon, F. Marias, C. Aymonier and M. Mench, *Biomass Bioenergy*, 2011, **35**, 872–883.
17 Y. Jian-guang, L. Jun-yuan, Y. Jian-ying, Z. Xu-liang and D. Zi-xiang, *J. Environ. Chem. Eng.*, 2014, **2**, 1358–1364.
18 X. Zhu, F. Qian, C. Zhou, L. Li, Q. Shi, S. Zhang and J. Chen, *Environ. Sci. Technol.*, 2019, **53**, 6580–6586.
19 F. Qian, X. Zhu, Y. Liu, Q. Shi, L. Wu, S. Zhang, J. Chen and Z. J. Ren, *Environ. Sci. Technol.*, 2018, **52**, 2225–2234.
20 J. Chen, *Bioresour. Technol.*, 2018, **265**, 320–327.
21 W. Dastyar, A. Raheem, J. He and M. Zhao, *Chem. Eng. J.*, 2019, **358**, 759–785.
22 Y. Wang, W. Deng, B. Wang, Q. Zhang, X. Wan, Z. Tang, Y. Wang, C. Zhu, Z. Cao and G. Wang, *Nat. Commun.*, 2013, **4**, 2141.
23 Y. Wang, H. Wang, H. Lin, Y. Zheng, J. Zhao, A. Pelletier and K. Li, *Biomass Bioenergy*, 2013, **59**, 158–167.
24 Z. Zhu, S. S. Toor, L. Rosendahl and G. Chen, *Environ. Prog. Sustainable Energy*, 2014, **33**, 737–743.
25 B. de Caprariis, P. De Filippis, A. Petrullo and M. Scarsella, *Fuel*, 2017, **208**, 618–625.
26 Z. Zhu, L. Rosendahl, S. S. Toor, D. Yu and G. Chen, *Appl. Energy*, 2015, **137**, 183–192.
27 M. N. Islam, G. Taki, M. Rana and J.-H. Park, *Ind. Eng. Chem. Res.*, 2018, **57**, 4779–4784.
28 J. Lu, Z. Liu, Y. Zhang and P. E. Savage, *ACS Sustainable Chem. Eng.*, 2018, **6**, 14501–14509.
29 Y. Yu, X. Lou and H. Wu, *Energy Fuels*, 2007, **22**, 46–60.
30 A. A. Peterson, F. Vogel, R. P. Lachance, M. Fröling, M. J. Antal Jr and J. W. Tester, *Energy Environ. Sci.*, 2008, **1**, 32–65.
31 C. Xu and N. Lad, *Energy Fuels*, 2007, **22**, 635–642.
32 Y. H. Chan, S. Yusup, A. T. Quitain, Y. Uemura and M. Sasaki, *J. Supercrit. Fluids*, 2014, **95**, 407–412.
33 T. H. Pedersen and L. A. Rosendahl, *Biomass Bioenergy*, 2015, **83**, 206–215.
34 R. Singh, A. Prakash, S. K. Dhiman, B. Balagurumurthy, A. K. Arora, S. Puri and T. Bhaskar, *Bioresour. Technol.*, 2014, **165**, 319–322.
35 M. K. Jindal and M. K. Jha, *RSC Adv.*, 2016, **6**, 41772–41780.
36 R. Li, B. Li, T. Yang, X. Kai, W. Wang, Y. Jie, Y. Zhang and G. Chen, *Bioresour. Technol.*, 2015, **198**, 94–100.
37 X.-F. Wu, Q. Zhou, M.-F. Li, S.-X. Li, J. Bian and F. Peng, *Bioresour. Technol.*, 2018, **270**, 216–222.
38 H. Li, S. Feng, Z. Yuan, Q. Wei and C. C. Xu, *Ind. Crops Prod.*, 2017, **109**, 426–433.
39 P. Das, T. Sreelatha and A. Ganesh, *Biomass Bioenergy*, 2004, **27**, 265–275.
40 Z. Zhu, B. Si, J. Lu, J. Watson, Y. Zhang and Z. Liu, *Bioresour. Technol.*, 2017, **243**, 9–16.
41 X. Peng, X. Ma, Y. Lin, J. Wang, X. Wei and X. Chen, *Bioresour. Technol.*, 2017, **238**, 510–518.
42 A. Demirbas, *Energy Sources, Part A*, 2010, **32**, 1100–1110.
43 A. Marcilla, L. Catalá, J. C. García-Quesada, F. Valdés and M. Hernández, *Renewable Sustainable Energy Rev.*, 2013, **27**, 11–19.
44 Z. Liu, A. Quek, S. K. Hoekman and R. Balasubramanian, *Fuel*, 2013, **103**, 943–949.
45 L. Leng, X. Yuan, H. Huang, J. Shao, H. Wang, X. Chen and G. Zeng, *Appl. Surf. Sci.*, 2015, **346**, 223–231.
46 O. Norouzi, F. Safari, S. Jafarian, A. Tavasoli and A. Karimi, *Energy Convers. Manage.*, 2017, **141**, 63–71.
47 T. G. Madenoğlu, M. Sağlam, M. Yüksel and L. Ballice, *J. Supercrit. Fluids*, 2016, **115**, 79–85.
48 T. G. Madenoğlu, M. Sağlam, M. Yüksel and L. Ballice, *J. Supercrit. Fluids*, 2013, **73**, 151–160.
49 M. Rashidi and A. Tavasoli, *J. Supercrit. Fluids*, 2015, **98**, 111–118.
50 N. Ü. Cengiz, S. Eren, M. Sağlam, M. Yüksel and L. Ballice, *J. Supercrit. Fluids*, 2016, **107**, 243–249.